Available online at www.sciencedirect.com

SciVerse ScienceDirect

Journal of Nutritional Biochemistry 23 (2012) 60–68

Journal of Nutritional Biochemistry

Dietary supplementation with dried plum prevents ovariectomy-induced bone loss while modulating the immune response in C57BL/6J mice☆

Elizabeth Rendina[a], Yin F. Lim[a], Denver Marlow[b], Yan Wang[a], Stephen L. Clarke[a], Solo Kuvibidila[a], Edralin A. Lucas[a], Brenda J. Smith[a,*]

[a]Department of Nutritional Sciences, Oklahoma State University, Stillwater, OK 74078, USA
[b]Department of Animal Resources, Oklahoma State University, Stillwater, OK 74078, USA

Received 12 March 2010; received in revised form 13 July 2010; accepted 12 October 2010

Abstract

This study was designed to investigate the effects of dried plum on the changes in bone metabolism and the immune response associated with ovarian hormone deficiency. Adult female C57BL/6J mice were either sham-operated (Sham) and fed AIN-93 diet (control) or ovariectomized (OVX) and fed a control diet with 0%, 5%, 15% or 25% dried plum (w/w), corresponding to control, low- (LDP), medium- (MDP) and high (HDP)-dose dried plum. Four weeks of HDP supplementation prevented the decrease in spine bone mineral density and content induced by OVX. The OVX compromise in trabecular bone of the vertebra and proximal tibia was prevented by the higher doses of dried plum, and in the vertebra these effects resulted in greater ($P<.05$) bone strength and stiffness. In the bone marrow, OVX suppressed granulocyte and committed monocyte populations and increased the lymphoblast population, but the MDP and HDP restored these myeloid and lymphoid populations to the level of the Sham. Dried plum also suppressed lymphocyte tumor necrosis factor (TNF)-α production *ex vivo* by splenocytes, in response to concanavalin (Con) A stimulation. These data indicate that dried plum's positive effects on bone structural and biomechanical properties coincide with the restoration of certain bone marrow myeloid and lymphoid populations, and suppressed splenocyte activation occurring with ovarian hormone deficiency.

Keywords: Osteoporosis; Ovariectomized; Dried plum; Osteoimmunology

1. Introduction

Osteoporosis continues to be a significant public health problem in the US with estimates that four out of 10 Caucasian women (≥50 years) will experience a fracture of the hip, spine or wrist [1]. In 2004, the Surgeon General's report highlighted the need for timely prevention, screening, diagnosis and treatment of osteoporosis and osteoporosis-related fractures across the lifespan [2]. Over the past two decades, significant advances have been made in the treatment of osteoporosis with Food and Drug Administration approval of anti-resorptive agents such as bisphosphonates and, more recently, the anabolic agent, intermittent parathyroid hormone therapy [2]. While these pharmacological options have significantly improved osteoporosis treatment, identifying lifestyle factors such as appropriate exercise regimens or foods with bioactive compounds that can prevent or delay bone loss could reduce the need for pharmacological therapies and the incidence of this debilitating condition.

Previously, dietary supplementation with dried plums (*Prunus domestica* L.) has been shown to protect against and reverse bone loss in gonadal hormone-deficient rat models of osteoporosis [3–6]. These studies demonstrated that dried plum's ability to preserve or restore bone mineral density (BMD) was associated with enhanced trabecular bone microarchitecture and improved biomechanical properties [3–6]. Although dried plums' bioactive component(s) responsible for these osteoprotective effects remains to be established, this fruit is a rich source of several nutrients and non-nutritive compounds, such as potassium, vitamin K, oligosaccharides and polyphenolic compounds, that may influence bone metabolism [7–10]. We have recently reported that an extract of the polyphenolic compounds from dried plums stimulates osteoblast calcified nodule formation *in vitro* by up-regulating key transcription factors involved in osteoblastogenesis (i.e., runt-related protein 2 or Runx2 and Osterix) [11]. Additionally, this extract decreased osteoclastogenesis and osteoclast activity *in vitro*, under inflammatory and oxidative stress conditions [12]. The resulting suppression of osteoclast differentiation and activity was mediated in part by the down-regulation of the inflammatory mediators, tumor necrosis

☆ Financial support: This study was funded in part by the Oklahoma Center for the Advancement of Science and Technology [HR06-109] and the California Dried Plum Board.

* Corresponding author. Department of Nutritional Sciences, HES 420 Oklahoma State University, Stillwater OK 74078, USA. Tel.: +1 405 744-3866.
E-mail address: bjsmith@okstate.edu (B.J. Smith).

0955-2863/$ - see front matter © 2012 Elsevier Inc. All rights reserved.
doi:10.1016/j.jnutbio.2010.10.010

factor (TNF)-α and receptor activator for nuclear factor-κB ligand (RANKL) [12]. These *in vitro* findings suggest that the polyphenolic compounds in dried plum have both bone and immune cell modulating effects.

The link between the immune system and bone metabolism has evolved from the early observations that cytokine production (e.g., interleukin-6 or IL-6, IL-1 and TNF-α) and certain immune cell populations (e.g., monocytes and T cells) were altered in conjunction with bone loss in ovarian hormone deficiency [13–16]. Since that time, the mechanisms by which IL-6, IL-1, TNF-α and other pro-inflammatory cytokines and chemokines up-regulate osteoclastogenesis and osteoclast activity, and down-regulate osteogenesis have been further delineated [13,17,18]. Furthermore, the role of myeloid and lymphoid cell populations in bone metabolism has also been recognized. For example, osteoclasts differentiate from myeloid progenitor cells at various stages of their lineage allocation similar to monocytes and neutrophils, and are up-regulated under inflammatory conditions [19]. T cells appear to be a major source of increased TNF-α in the bone marrow of oophorectomized animals [20]. Moreover, activated T cells serve as one of the primary sources of the osteoclast differentiation factor, RANKL, and B cells produce a significant proportion of RANKL's decoy receptor, osteoprotegerin (OPG), in the bone marrow [21,22]. Thus, it is apparent that immune cells and their mediators contribute to the regulation of bone turnover.

Due to evidence demonstrating the potent anti-inflammatory properties of dried plum's polyphenols *in vitro* [12], this study was designed to determine whether dietary supplementation with dried plum alters the immune response while protecting against bone loss in gonadal hormone-deficient adult mice. We hypothesized that dried plum would dose-dependently attenuate the ovariectomy-induced alterations in immune cell populations and their response to an immunological challenge coincident with protecting against bone loss. Previous animal studies with dried plum have focused on rat models of osteoporosis; hence, this study is the first to evaluate the effects of dried plum in preventing ovarian hormone deficiency-induced bone loss utilizing the C57BL/6J mouse, a well-characterized model for immunological studies.

2. Materials and methods

2.1. Animal care

Fifty-nine female 12-week-old C57BL/6J mice (Jackson Labs, Bar Harbor, ME, USA) were housed in an environmentally controlled laboratory animal research facility. Following a 7-day acclimation period, all mice were anesthetized using a ketamine/xylazine cocktail (80 mg ketamine and 8 mg xylazine/kg body weight) for either a sham operation (Sham) or bilateral oophorectomy (OVX), and randomly assigned to one of five treatment groups (n=9-10 mice/group): Sham control diet (AIN-93), OVX control diet or OVX consuming control diet supplemented with 5% [low-dose (LDP)], 15% [medium-dose (MDP)] or 25% [high-dose (HDP)] w/w dried plum for 4 weeks. These doses were selected to evaluate dried plum's influence on the osteoimmunological response in the C57BL/6J mouse based on their efficacy in preventing bone loss in rat models of osteoporosis [3,4,6].

Immediately following surgery, mice were individually housed to allow for postsurgical recovery and started on their respective dietary treatments. All diets were adjusted for macronutrient, calcium, phosphorus and fiber content (Table 1). The amount of food fed to the OVX animals was matched to the mean consumption of the Sham animals, and body weights were recorded weekly. After 4 weeks of treatment, mice were anesthetized using the same ketamine/xylazine cocktail described above and exsanguinated via the carotid artery. A 25-μl aliquot of blood was taken for total white cell counts. The remaining blood was collected in EDTA-coated tubes, centrifuged at 730×g for 20 min at 4°C and plasma aliquots stored at −80°C for biochemical marker analyses. Femurs were cleaned of soft adhering tissue and the bone marrow was immediately flushed from one femur with ice-cold phosphate buffered saline (PBS) for flow cytometry and the other femur was snap frozen for gene expression analyses. The spines were trimmed of soft tissue and stored at −20°C. Spleens were harvested and immediately placed in sterile, ice-cold PBS for *ex vivo* experiments.

Table 1
Diet composition

Ingredients	Control	LDP	MDP	HDP
	(g/kg diet)			
Dried plum	0	50	150	250
Carbohydrate				
Cornstarch	465.7	427.09	349.86	273.63
Maltodextrin	155	155	155	155
Sucrose	100	100	100	100
Dried plum	0.00	38.62	115.85	193.08
Protein				
Casein	140	137.53	132.59	127.65
Dried plum	0.00	2.47	7.41	12.35
Fat				
Soybean oil	40	38.91	36.73	34.55
Dried plum	0.00	1.09	3.27	5.45
Fiber				
Cellulose	50	48.88	46.63	44.38
Dried plum	0.00	1.13	3.38	5.63
Vitamin mix	10	10	10	10
Mineral mix				
Mineral mix (Ca and P deficient)	13.4	13.4	13.4	13.4
Calcium carbonate	12.5	12.48	11.85	11.43
Calcium from dried plum	0.00	0.09	0.26	0.43
Sodium phosphate, monobasic (NaH_2PO_4)	5.6	5.39	5.3	5.09
Potassium phosphate, monobasic (KH_2PO_4)	2.4	2.32	2.28	2.19
Phosphorus from dried plum	0.00	0.05	0.16	0.27
Sucrose	1.1	1.27	1.76	2.22
Choline bitartrate	2.50	2.50	2.50	2.50
L-Cysteine	1.80	1.80	1.80	1.80

Control diet is AIN-93M.

2.2. Bone densitometry assessment

The excised spine was scanned using dual-energy X-ray absorptiometry (DXA; LunarPIXI, GE Medical Systems, Madison, WI, USA) to determine bone mineral area (BMA), content (BMC) and density (BMD) of the fourth to fifth lumbar vertebrae (L4–5). All DXA scans were analyzed using PIXImus Series Software version 1.4x.

2.3. Microcomputed tomography analyses

The tibia and fourth lumbar vertebra were scanned using microcomputed tomography (μCT40, SCANCO Medical, Switzerland) to assess bone microarchitecture at two different skeletal sites. The proximal tibial metaphysis and mid-diaphysis were used to analyze trabecular and cortical bone in a long bone. Tibial scans of the proximal tibia metaphysis were performed at a resolution of 2048×2048 pixels. Analysis of the proximal tibia was accomplished by placing semi-automated contours starting 30 μm distal to the growth plate and included a 600-μm volume of interest (VOI) of only secondary spongiosa for trabecular analyses. Trabecular parameters evaluated included bone volume expressed per unit of total volume (BV/TV), trabecular number (TbN), trabecular thickness (TbTh), trabecular separation (TbSp), connectivity density (ConnDens) and structural model index (SMI). For cortical bone analysis, cortical porosity, thickness, area and medullary area of the tibial mid-diaphysis were evaluated by analyzing 120 μm at the mid-point of the tibia.

Vertebral analyses were performed by acquiring images at a resolution of 1024×1024 pixels, 30 μm from the dorsal and caudal growth plates. Similar to the tibial analysis, semi-automated contours were placed to assess secondary spongiosa within the VOI. All analyses were performed at a threshold of 300 and a sigma and support of 1.2 and 2.0, respectively.

2.4. Biomechanical testing of vertebra with finite element analysis

Reconstructed 3-D images were used to evaluate the alterations in biomechanical properties of trabecular bone using finite element (FE) analysis software (SCANCO Medical). A micromechanical FE model was constructed by converting voxels from the VOI into eight-node brick elements [23]. The elements in this FE model had linear, elastic and isotropic material properties. Compression testing was simulated on trabecular regions of the vertebral body and tibial metaphysis. Total force, stiffness, size-independent stiffness and von Mises stresses were determined.

2.5. Plasma PINP and IGF-I

To provide further insight into the alterations in bone metabolism associated with dried plum, plasma N-terminal propeptide of type I procollagen (PINP) as an indicator of bone formation and insulin-like growth factor (IGF)-1 were determined

using commercially available kits according to the manufacturer's specifications (Immunodiagnostic Systems, Inc., Fountain Hills, AZ, USA). The inter- and intra-assay coefficient of variations for PINP were 9.2% and 6.4%, and for IGF-1 were 8.8% and 7.3%, respectively.

2.6. RNA Extraction and quantitative real-time PCR

Quantitative real-time PCR (qRT-PCR) analyses were used to evaluate the alterations in bone mRNA levels of genes associated with osteoblast and osteoclast differentiation and activity (i.e., Runx2, OCN, NFATc1). Whole mouse femurs were pulverized (Spex 6770 freezer mill) and total RNA extracted from homogenized bone using Trizol Reagent (Life Technology, Rockville, MD, USA). RNA was further purified using the RNeasy MinElute Kit (Qiagen, Valencia, CA, USA), and the A_{260}/A_{280} ratio was obtained using a Nanodrop Spectrophotometer (Rockland, DE, USA) to determine the quantity and quality of RNA. qRT-PCR was then performed using 2 μg of total RNA pretreated with DNase I and subjected to reverse transcription (Superscript II, Invitrogen, Carlsbad, CA, USA). cDNA (50 ng) was used for each qRT-PCR reaction and all reactions were assayed in duplicate using SYBR green chemistry (Roche, Penzberg, Germany) on the Applied Biosystems 7900HT Fast Real-Time PCR System (Foster City, CA, USA). The following primers were used: nuclear factor for activated T cells cytoplasmic 1 (NFATc1), 5′-GCG AAG CCC AAG TCT CTT TCC-3′ and 5′-GTA TGG ACC AGA ATG TGA-3′; Runx2, 5′-CGA CAG TCC CAA CTT CCT GT-3′ and 5′-CGG TAA CCA CAG TCC CAT CT-3′; osteocalcin (OCN), 5′-TGA GCT TAA CCC TGC TTG TGA CGA-3′ and 5′-AGG GCA CAG GTC CTA AAT AGT-3′; and hypoxanthine guanine phosphoribosyltransferase 1 (HPRT1), 5′-GCC TAA GAT GAG CGC AAG TTG-3′ and 5′-TAC TAG GCA GAT GGC CAC AGG-3′. All qRT PCR results were evaluated by the comparative cycle number at threshold (C_T) method using HPRT1 as the invariant control.

2.7. Myeloid and lymphoid populations

Evaluation of bone marrow myeloid and lymphoid populations was accomplished using flow cytometry techniques. At the time of harvest, bone marrow cells were kept on ice and then centrifuged at 180×*g* for 5 min at 4°C. After centrifugation, PBS was aspirated and cells were resuspended in lysing buffer (BD Biosciences, Franklin Lakes, NJ, USA) for 9 min at room temperature. The cells were washed and resuspended in 10 ml of DMEM media containing 0.5% bovine serum albumin (BSA) and 10 mM EDTA (pH 7.4) (Gibco/Invitrogen, Carlsbad, CA, USA), counted and the concentrations adjusted to 1×10^6 cells/ml. For the analyses, aliquots of 1×10^5 cells were incubated with normal mouse serum FcBlock (BD Biosciences) on ice for 15 min prior to incubation with the antibodies. The following antibodies were then added at predetermined dilutions and incubated on ice for 20 min: Ly-6C, CD11b, CD31, CD4 and CD8 (BD Biosciences) and CD115, CD19 and CD3 (eBioscience, San Diego, CA, USA). Following incubation with the antibodies, samples were washed twice with 350 μl PBS/0.5% BSA/20 mM sodium azide and centrifuged at 180×*g* for 5 min at 4°C. Following the second wash, the cells were resuspended in 350 μl of PBS/0.5% BSA/20 mM sodium azide and sorted using a Becton Dickinson FACSCalibur. Cells were characterized based on the following cell surface markers: granulocyte ($CD31^{-}Ly\text{-}6C^{+}$), mature myeloid cells ($CD11b^{+}$), committed monocytes ($CD115^{+}$), monocytes ($CD31^{-}Ly\text{-}6C^{hi}$), lymphoid cells ($CD31^{+}Ly\text{-}6C^{-}$), myeloid progenitor cells ($CD31^{+}Ly\text{-}6C^{+}$), lymphoblasts ($CD31^{hi}Ly6C^{-}$), B cells ($CD19^{+}$), T cells ($CD3^{+}$) and helper T cells ($CD3^{+}CD4^{+}$). Data were analyzed using Summit software version 4.3 (Dako Colorado, Inc., Fort Collins, CO, USA).

2.8. Ex vivo cytokine analyses with splenocytes

To evaluate the immune cellular response to mitogen challenge, single cell suspensions were prepared as previously reported [24]. Briefly, spleens were removed under aseptic conditions and immediately transferred to culture tubes containing 1 ml wash medium (PBS with 2.5% fetal calf serum or FCS, 100 μg/ml streptomycin and 100 U penicillin/ml). Each spleen was gently homogenized in a cell strainer and the strainer was rinsed with 10 ml wash medium. Cell suspensions were centrifuged at 260×*g* at 4°C for 10 min and the pellets were treated with 1 ml sterile, ice-cold deionized water for 20-30 s to lyse the red blood cells. After lysing, 9 ml of wash buffer was added and a second centrifugation under the same conditions followed. Cell pellets were then resuspended in 3 ml of culture medium consisting of RPMI-1640 supplemented with 10% FCS, 2 mM L-glutamine, 1 mM nonessential amino acids, 1 mM sodium pyruvate, 100 U/ml penicillin, 100μg/ml streptomycin and 50 μM β-mercaptoethanol. Total and viable cell counts were performed by standard techniques under light microscope.

Macrocultures were prepared by plating 2×10^6 viable, nucleated cells/well in a 24-well plate as previously described [25]. Cells were then treated with lipopolysaccharide (LPS) (2.5 μg/ml), Con A (2.5μg/ml) or culture medium as a control. Plates were incubated at 37°C, 5% CO_2 in a humidified incubator for 48 h. At the end of incubation period, the cultures were centrifuged at 260×*g* for 10 min at 4°C. The supernatant was immediately frozen at −80°C until cytokine assay. IL-6 and TNF-α in the supernatant were measured using commercially available ELISA kits (BD Biosciences). The intra- and inter-assay coefficients of variation for IL-6 were <6.4 and <4.0, while for TNF-α were <9.5 and <7.6, respectively.

2.9. Statistical analysis

Statistical analysis was accomplished using SAS version 9.1 (SAS Institute, Cary, NC, USA). One-way ANOVA was performed using proc glm followed by *post hoc* analysis with Fisher's least square means separation test when *F* values were significant. All data are presented as mean±S.E. and the α was set at .05.

3. Results

3.1. Body weight and composition, food intake and uterine weight

At baseline, body weights were similar amongst all groups. Despite no intergroup differences in food intake, the OVX groups experienced significant weight gain by the end of the 4-week study compared to the Sham cohort (Table 2). No significant differences were observed in lean body mass due to OVX; however, fat mass and percent fat were significantly increased (Table 2). The fat mass of the HDP cohort was similar to the Sham, which indicated the prevention of the OVX-induced increase in percent of body fat. Bilateral oophorectomy was deemed successful and no estrogenic effects of dried plum were observed based on significant atrophy of the uterus with all OVX groups experiencing an ~80% decrease in uterine weight compared to Sham (Table 2).

Table 2
Body and tissue weights, food intake, body composition and spine BMA and BMC following 4 weeks of treatment

	Sham	OVX	LDP	MDP	HDP
Body weight					
Baseline (g)	19.5±0.3	19.8±0.4	19.7±0.3	19.6±0.5	19.5±0.4
Final (g)	19.5±0.3^{b}	21.4±0.4^{a}	21.7±0.3^{a}	21.4±0.2^{a}	21.9±0.3^{a}
Food intake (g/day)	5.0±0.2	4.4±0.2	4.5±0.2	4.4±0.2	4.5±0.2
Body composition					
Fat (g)	4.9±0.1^{c}	5.6±0.1^{ab}	5.8±0.3^{a}	5.5±0.1^{ab}	5.3±0.1^{ac}
Lean (g)	13.8±0.4	14.4±0.2	14.0±0.3	13.9±0.1	14.4±0.4
Fat (%)	26.3±0.3^{b}	28.2±0.5^{a}	29.2±0.5^{a}	28.4±0.4^{a}	26.8±0.4^{b}
Uterine weight (mg)	97.0±16.0^{a}	19.0±3.0^{b}	21.0±3.0^{b}	21.0±5.0^{b}	21.0±2.0^{b}
Total WBC (1×10^3)	4425.0±585.3^{b}	6627.8±281.9^{a}	5459.1±594.0^{b}	5942.7±421.9^{b}	5240.0±430.9^{b}
Spine bone densitometry					
BMA (cm^2)	0.418±0.005	0.414±0.005	0.420±0.003	0.414±0.003	0.420±0.004
BMC (g)	0.021±0.0004^{a}	0.019±0.0005^{b}	0.019±0.0003^{b}	0.019±0.0003^{b}	0.020±0.0005^{a}
BMD (g/cm^2)	0.050±0.0008^{a}	0.046±0.0007^{b}	0.045±0.0005^{b}	0.046±0.0004^{b}	0.048±0.0008^{a}

Sham and OVX groups consumed control diet (AIN-93M). All other OVX groups consumed either the LDP, MDP or HDP diet.
Values are means±S.E. Within a given row, values that do not share the same superscript are significantly different ($P<.05$) from each other.

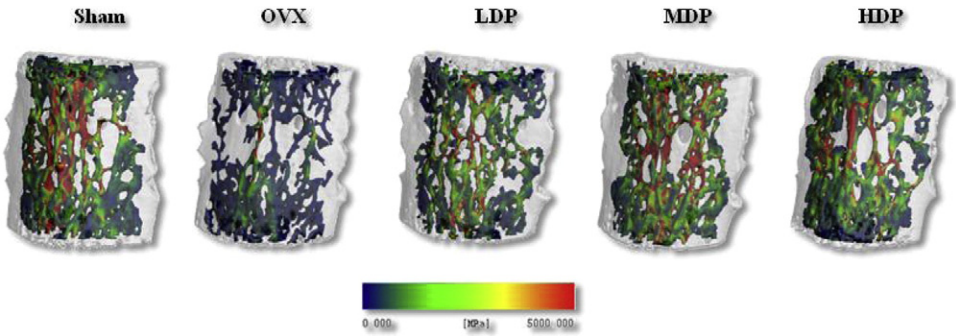

Fig. 1. Representative 3-D μCT images are shown of the vertebral body trabeculae with the correspondning biomechanical properties (total force) based on FE analysis for Sham, OVX and OVX animals consuming the 5% (LDP), 15% (MDP) or 25% (HDP) diets. Images are color coded based on a scale indicating the force (MPa) with blue associated with weaker points and moving through the color spectrum to red which is associated with stronger points within the trabecular structure.

3.2. Total white cell counts

Total white cell counts in the peripheral blood were elevated in response to ovarian hormone deficiency and this increase was attenuated by all three doses of dried plum (Table 2).

3.3. Spine bone mineral area, content and density

DXA scans revealed that OVX animals on control diet had an 8% lower BMD compared to the Sham group after 4 weeks (Table 2). The HDP prevented the loss of spine BMD associated with OVX, but the two lower doses of dried plum (i.e., LDP and MDP) were unable to achieve this effect. Preservation of BMC in animals receiving the HDP diet accounts for the effects on BMD and no differences were observed between groups in BMA.

3.4. Trabecular and cortical bone microarchitecture

Representative three-dimensional images generated by the μCT analysis of the vertebral body are shown for each group with the trabecular structures color coded to reflect the biomechanical properties of the specimen as determined by FE analyses (Fig. 1). In the OVX cohort, vertebral BV/TV of the trabecular bone was decreased by ~20% over the 4-week study period compared to the Sham cohort (Fig. 2A). The two higher doses of dried plum (i.e., MDP and HDP) were able to prevent the decrease in BV/TV due to

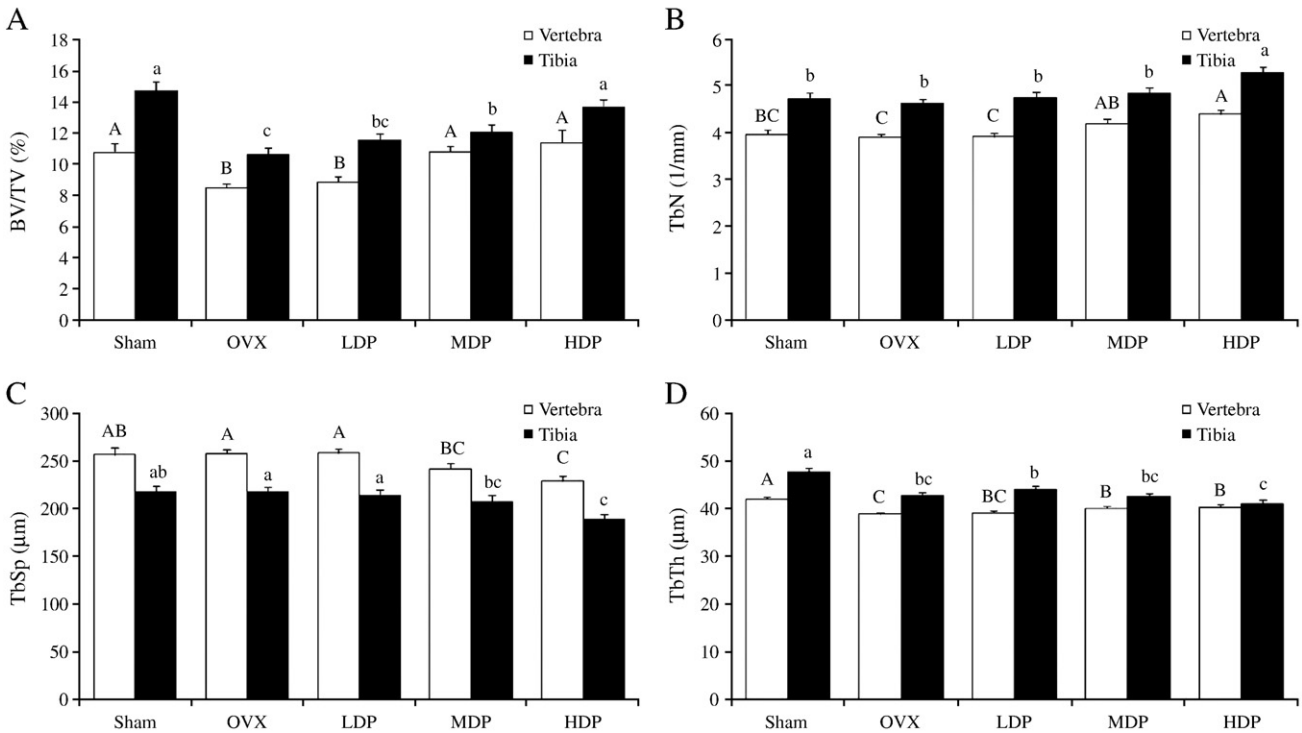

Fig. 2. Comparisons of trabecular bone morphometric parameters in sham-operated (Sham) and ovariectomized (OVX) mice fed control diet or control diet supplementated with either 5% (LDP), 15% (MDP) or 25% (HDP) dried plum. Bone microarchitectural parameters include (A) bone volume/total volume (BV/TV), (B) trabecular number (TbN), (C) trabecular separation (TbSp) and (D) trabecular thickness (TbTh). Bars for either the vertebra (black bars) or tibia (white bars) that share the same upper- or lowercase superscript letter are not significantly different from each other ($P<.05$).

Table 3
Non-morphometric trabecular and cortical bone microarchitectural parameters of the vertebra and tibia

	Sham	OVX	LDP	MDP	HDP
Vertebra					
ConnDens	95.52±9.2^{bc}	75.46±3.0^{c}	79.07±5.0^{c}	114.20±7.6^{ab}	125.87±13.3^{a}
SMI	2.281±0.05^{b}	2.546±0.03^{a}	2.511±0.04^{ab}	2.327±0.042^{b}	2.317±0.09^{b}
Apparent mean/density	1.36±0.02^{bc}	1.32±0.01^{c}	1.33±0.01^{c}	1.40±0.02^{bc}	1.42±0.03^{a}
Tibia					
ConnDens	197.10±20.6^{ab}	154.28±9.8^{b}	161.95±15.7^{b}	178.92±11.2^{b}	230.39±22.6^{a}
SMI	1.84±0.08^{c}	2.39±0.05^{a}	2.31±0.04^{a}	2.23±0.07^{ab}	2.09±0.07^{b}
Apparent mean/density	217.67±6.18^{a}	166.38±4.55^{d}	178.46±4.43^{cd}	184.65±5.43^{c}	202.23±4.59^{b}
Cortical					
Cortical thickness (mm)	0.202±0.002	0.196±0.002	0.195±0.002	0.196±0.002	0.197±0.002
Cortical area (mm^2)	0.56±0.01	0.568±0.01	0.574±0.01	0.568±0.01	0.564±0.01
Medullary area (mm^2)	0.771±0.02	0.827±0.03	0.846±0.04	0.85±0.04	0.812±0.03
Porosity (%)	57.67±0.5	59.09±0.5	59.35±0.7	59.71±0.7	58.74±0.7

Sham and OVX groups consumed control diet. All other OVX groups consumed either the LDP, MDP or HDP diet.
Values are means±S.E., n=8 in each group. Within a row, values that do not share the same superscript are significantly different (P<.05) from each other.

OVX resulting in trabecular bone volume that was comparable to that of the Sham group (Fig. 2A). OVX did not significantly alter vertebral TbN or TbSp, but HDP increased TbN and decreased TbSp beyond that of the Sham control group (Fig. 2B and C). TbTh of the vertebra was decreased by OVX compared to Sham-operated animals, and the cohorts on the MDP and HDP diets experienced an increase in TbTh compared to OVX suggesting that the effects on BV/TV were a result of increased thickness of the trabeculae (Fig. 2D). Although at 4 weeks postsurgery no significant decreases in connectivity density were observed between the Sham and OVX groups, the HDP and MDP enhanced trabecular bone connectivity density compared to the OVX controls and the HDP increased connectivity density to a level greater than that in the Sham group (Table 3). The SMI, which distinguishes a weaker rod-like structure from a stronger plate-like structure, indicated that vertebral specimens from OVX animals were more rod-like (i.e., increasing values), whereas the Sham and HDP group were more plate-like (i.e., SMI closer to 0) (Table 3).

Similar to the observations in the vertebra, the OVX group on control diet had significantly reduced tibial BV/TV (29.7%) after 4 weeks, and the MDP and HDP treatments prevented this loss of trabecular bone (Fig. 2A). No significant OVX-induced changes in TbN or TbSp were observed in the tibia of the OVX group, but the HDP group had a higher TbN (Fig. 2B) and lower TbSp (Fig. 2C) compared to the Sham group. More modest benefits in tibial TbN and TbSp were observed with the MDP treatment. OVX significantly decreased TbTh of the tibia compared to Sham animals, and none of the dried plum treatments was able to protect against this phenomenon (Fig. 2D). Based on the alterations in morphometric parameters in the tibial metaphysis, HDP resulted in a greater connectivity density and improved SMI to a more plate-like structural arrangement (Table 3).

Cortical bone assessed at the tibial mid-diaphysis indicated that cortical thickness, cortical area, medullary area and cortical porosity were not altered in response to OVX or dietary treatments (Table 3).

3.5. Biomechanical properties of trabecular bone

Finite element analyses indicated that the alterations in trabecular microarchitecture due to OVX resulted in decreased total force, stiffness and size-independent stiffness of the vertebra compared to Sham animals. As may have been anticipated based on the structural changes, the MDP and HDP diets prevented the compromise in the bone biomechanical properties, including total force, stiffness and size-independent stiffness (Table 4). Von Mises stress distribution, which is usually negatively correlated with BV/TV, increased in OVX cohort compared to Sham, and the MDP and HDP diets protected against these changes (Table 4). In the proximal tibial metaphysis, the alterations in trabecular bone microarchitectural properties due to OVX and treatments at 4 weeks were not of the magnitude to produce significant changes in any of the biomechanical properties that were assessed (Table 4).

3.6. Plasma biochemical markers

Plasma PINP and IGF-1 were increased in the OVX animals on control diet compared to the Sham group, indicating that bone formation increased with ovarian hormone deficiency (Fig. 3A and B). All doses of dried plum restored plasma PINP to the level of the Sham (Fig. 3A). The OVX-induced increase in plasma IGF-1 was further elevated in the MDP group (P<.05), but not with either of the LDP or HDP treatment (Fig. 3B).

Table 4
Biomechanical properties of trabecular bone in the lumbar vertebra and proximal tibial metaphysis

	Sham	OVX	LDP	MDP	HDP
Vertebra					
Total force (N)	29.74±5.5^{ab}	16.35±4.2^{c}	21.20±2.7^{bc}	39.69±4.8^{a}	40.20±4.6^{a}
Stiffness (1×10^3 N/m)	47.20±8.66^{a}	25.61±6.30^{b}	33.12±4.18^{b}	65.77±6.16^{a}	63.70±7.04^{a}
Size-independent stiffness (N/m)	90.21±17.0^{ab}	47.13±11.70^{c}	67.79±9.32^{bc}	116.51±17.80^{a}	121.78±15.0^{a}
Von Mises stresses	1.09±0.2^{b}	1.62±0.3^{a}	1.22±0.1^{ab}	0.85±0.1^{b}	0.82±0.1^{b}
Tibia					
Total force (N)	189.05±24.6	148.37±23.6	168.40±19.7	168.29±22.2	192.59±6.2
Stiffness (1×10^3 N/m)	1060.87±138.36	832.62±132.66	945.02±110.55	944.37±124.67	1080.73±34.61
Size-independent stiffness (N/m)	284.46±35.5	201.18±30.47	241.50±27.4	259.67±34.3	287.99±12.0
Von Mises stresses	6.93±0.4	9.18±1.2	8.56±1.3	8.7±1.1	7.07±0.4

Sham and OVX groups consumed control diet. All other OVX groups consumed either the LDP, MDP or HDP diet.
Values are means±S.E., n=8 specimen/group. Within a row, values that do not share the same superscript are significantly different (P<.05).

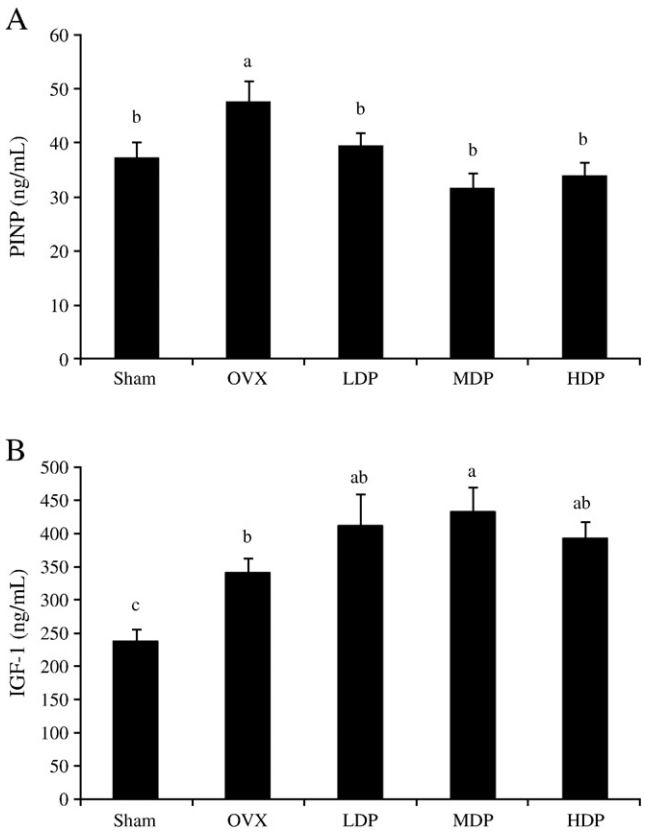

Fig. 3. Plasma biomarkers associated with bone metabolism following 4 weeks of treatments: (A) N-terminal propeptide of type I procollagen (PINP) and (B) insulin-like growth factor (IGF)-1. Bars that share the same superscript letter are not significantly different from each other ($P<.05$).

3.7. Femur gene expression

The relative expression of NFATc1, the key transcription factor that regulates osteoclastogenesis, was suppressed in the femur by the three doses of dried plum compared to the OVX animals on the control diet (Fig. 4A). All three doses of dried plum reduced the relative abundance of Runx2 (Fig. 4B) and the two higher doses suppressed OCN expression compared to the OVX controls (Fig. 4C). These data suggest that osteoblastogenesis and mineralization were also suppressed by dried plum in the femur of OVX animals.

3.8. Alterations in bone marrow myeloid and lymphoid populations

In terms of myeloid populations, OVX significantly reduced granulocyte ($CD31^{-}Ly\text{-}6C^{+}$) counts in the bone marrow compared to the Sham group and the two higher doses of dried plum (i.e., MDP and HDP) prevented this response (Fig. 5A). The number of committed monocytes ($CD115^{+}$) was also decreased with OVX, and only the HDP dried plum restored these cell counts to that of the Sham (Fig. 5B). All OVX groups experienced an increase in bone marrow monocytes ($CD31^{-}Ly\text{-}6C^{hi}$), but dried plum had no effect on this population (Fig. 5C). Even though the alterations in absolute lymphoblast ($CD31^{hi}Ly\text{-}6C^{-}$) counts in the OVX group consuming the control diet did not significantly increase compared to the Sham group, MDP and HDP decreased lymphoblast counts (Fig. 5D). No alterations in myeloid progenitor ($CD31^{+}Ly\text{-}6C^{+}$) and mature myeloid ($CD11b^{+}$) cells were observed in response to OVX and treatment (data not shown).

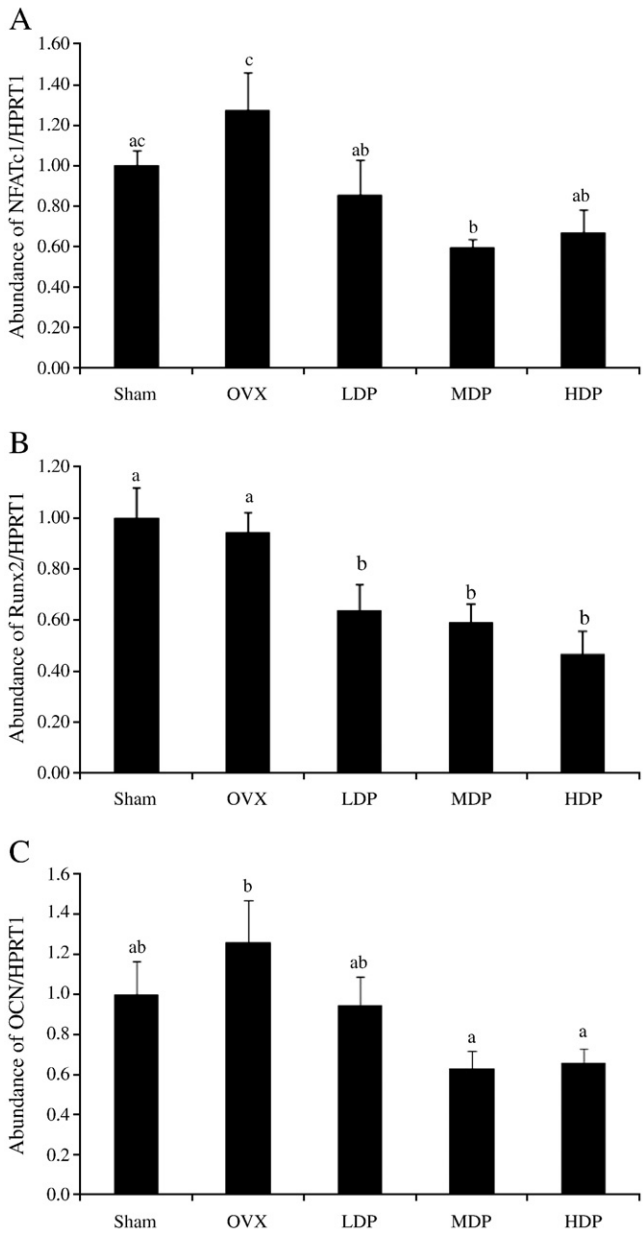

Fig. 4. Relative abundance of (A) NFATc1, (B) Runx2 and (C) OCN RNA in the femur of Sham, OVX and OVX animals consuming the 5% (LDP), 15% (MDP) or 25% (HDP) diets. HPRT1 was used as the invariant control. Bars represent the mean±S.E. Bars that share the same superscript letter are not significantly different from each other ($P<.05$).

Bone marrow lymphoid ($CD31^{+}Ly\text{-}6C^{-}$) and B cells ($CD19^{+}$) tended ($P<.10$) to increase with OVX, but the change did not reach the level of statistical significance (data not shown). $CD3+$ T cells and helper T cells ($CD3^{+}CD4^{+}$) were not altered due to ovarian hormone deficiency or any of the doses of dried plum.

3.9. Splenocyte cytokine production

Following Con A stimulation of splenocytes (i.e., T cell and monocyte co-cultures) *ex vivo*, TNF-α production was increased in cells from the OVX group by approximately 35% compared to cells from the Sham group (Fig. 6A). Both the MDP and HDP treatments protected against Con A-induced increase in TNF-α production associated with OVX. Secretion of IL-6 in response to Con A was not

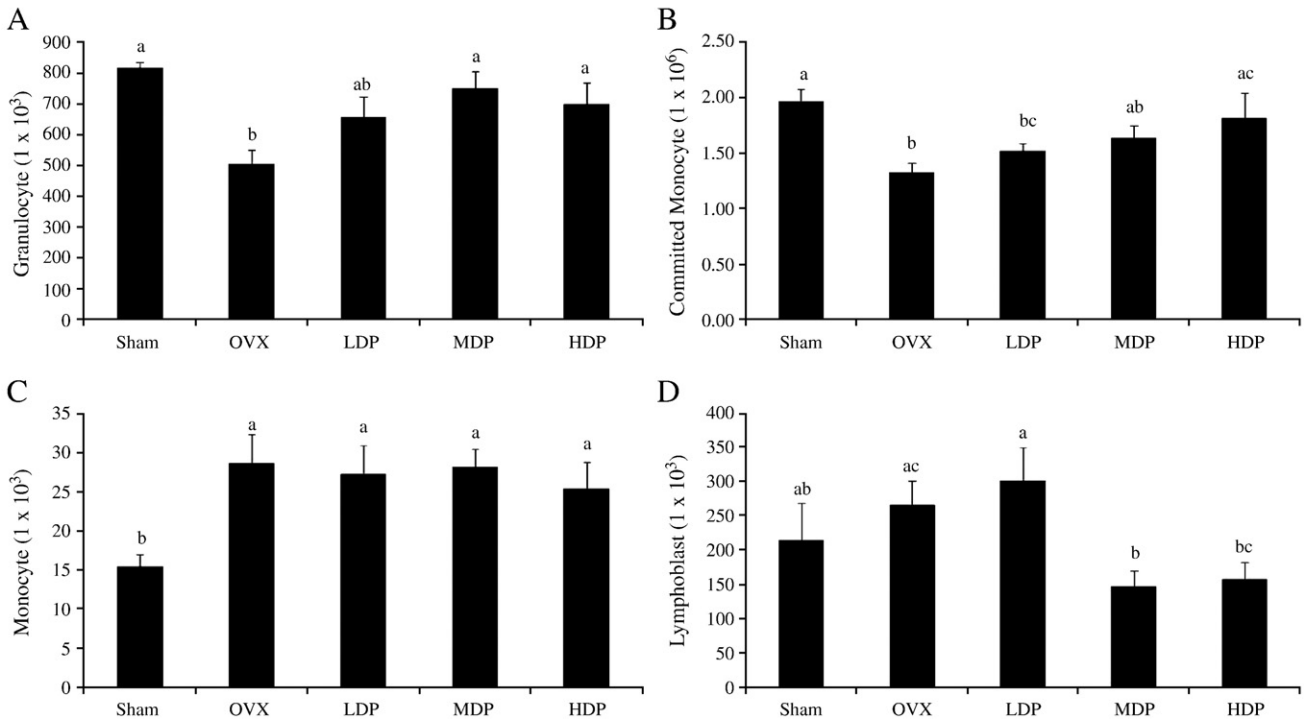

Fig. 5. Alterations in (A) granulocyte, (B) committed monocyte, (C) monocyte and (D) lymphoblast populations in the bone marrow of sham-operated (Sham) and ovariectomized (OVX) mice fed control diet or control diet supplementated with either 5% (LDP), 15% (MDP) or 25% (HDP) dried plum. Bars that share the same superscript letter are not significantly different from each other ($P<.05$).

significantly increased due to OVX or altered due to treatments (Fig. 6B). Neither IL-6 nor TNF-α production by splenocytes was altered with LPS stimulations (data not shown).

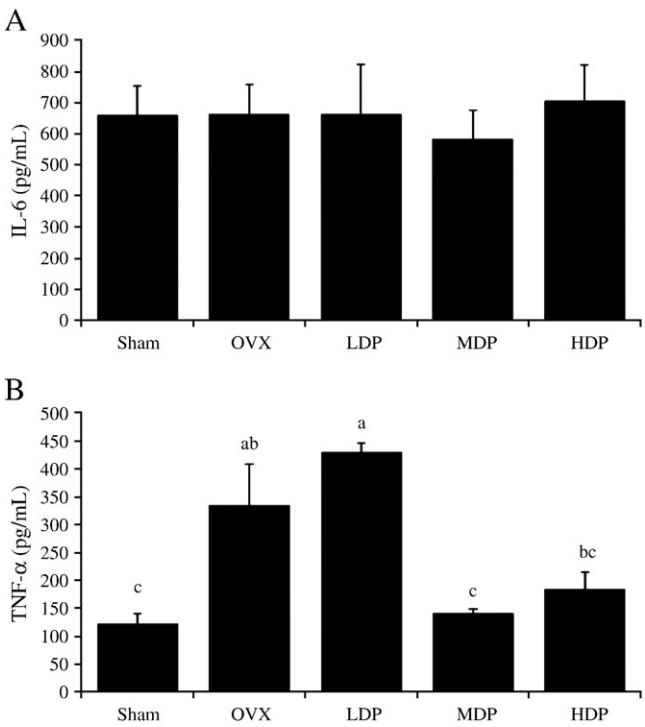

Fig. 6. Splenocyte production of TNF-α (A) and IL-6 (B) evaluated under *ex vivo* conditions. Splenocytes were harvested from each treatment group and challenged with ConA. Bars represent the mean±S.E. and bars that share the same superscript letter are not significantly different from each other ($P<.05$).

4. Discussion

The current study revealed that dried plum supplementation protected against bone loss induced by gonadal hormone deficiency in adult female C57BL/6J mice, similar to our previous observations in the Sprague-Dawley rat [3–6]. In particular, the two higher doses of dried plum (i.e., MDP and HDP) prevented the deterioration of trabecular bone microarchitectural brought about by OVX in the lumbar vertebra as well as the proximal tibial metaphysis. The benefit of the HDP diet on vertebral trabecular bone was such that the total vertebral bone mineral content was not altered by ovarian hormone deficiency resulting in the preservation of bone density. These results are similar to the findings from previous studies utilizing rat models of osteoporosis, in which the most pronounced alterations in BMD and trabecular bone microarchitecture were observed in the 25% dried plum diet and the 15% diet was the lowest effective dose [3,4]. Although these doses (i.e., 15% and 25% w/w) are not likely achievable through routine human consumption, understanding the underlying mechanism by which dried plum alters bone metabolism and ongoing efforts in our laboratories to determine the bioactive components may lead to the development of dietary supplements or cultivars of plums that provide a rich source of the bioactive components.

The protective effects of dried plum on bone mass and structural properties were associated with significantly lower levels of the bone formation marker, PINP, in the OVX groups consuming diets supplemented with dried plum. Furthermore, the suppression of Runx2 and OCN indicated that the differentiation of osteoblasts and the mineralization of bone were suppressed with the dried plum. This is the first study to suggest that dried plum suppresses the OVX-induced increase in bone formation after 4 weeks of treatment, which does not explain the restoration of bone mass in osteopenic animal models as previously reported [6]. Future studies should consider the kinetic response of bone to dried plum supplementation *in vivo* to provide an explanation for this response. Nonetheless, these

findings related to bone formation, combined with the decrease in bone NFATc1 expression, suggest that dried plum decreased osteoclastogenesis and osteogenesis in the OVX animals and, thus, suppressed the accelerated bone turnover associated with gonadal hormone deficiency. However, it remains to be determined whether dried plum had a greater influence on bone resorption or bone formation phase of bone remodeling.

Interestingly, in this study the alterations in bone metabolism observed in response to OVX and dried plum treatments coincided with alterations in bone marrow cell populations. FACS analysis on the bone marrow demonstrated that even though there were no alterations in mature myeloid or myeloid progenitor cells in response to OVX, granulocyte and committed monocyte decreased while monocytes increased. These data suggest that differentiation of myeloid cells into $CD31^{+}Ly\text{-}6C^{hi}$ monocytes is increased with OVX, which coincides with previous reports that monocyte–macrophage lineage cells are increased in ovarian hormone deficiency and suppressed with estrogen treatment [26]. Likewise, the decrease in the number of committed monocytes ($CD115^{+}$ or macrophage colony-stimulating factor receptor positive cells) in the OVX compared to Sham groups may reflect an increase in the differentiation of these cells into osteoclasts, but confirmational analyses of osteoclast precursor cells would be needed. Although dried plum treatment had no effect on bone marrow monocytes, it restored the granulocyte and committed monocyte populations to the level of the Sham animals. Thus, these findings combined with the gene expression data provide the initial evidence that dried plum decreases bone resorption *in vivo* by suppressing osteoclastogenesis in part by down-regulating NFATc1 similar to our previous reports *in vitro* [11,12]. Further studies are needed to confirm that dried plum alters actual osteoclasts and their precursors, as well as osteoblast lineage cells to better understand the stage of differentiation in which these changes occur *in vivo*.

Due to the contribution of T cells and B cells as potential source of RANKL and OPG and other contributing factors to osteoclastogenesis and osteogenesis, we also assessed the alterations in lymphoid populations in the bone marrow that occur in response to ovarian hormone deficiency and dried plum. Our data indicate that B cells and lymphoid populations tended to increase with ovarian hormone deficiency. This increase in lymphoid lineage cells has been previously reported in response to surgically induced ovarian hormone deficiency in both mouse and rat models. Furthermore, 17β-estradiol has been shown to reverse these effects [27–29]. Dried plum did not alter the number of any of these T- and B-lymphocyte subpopulations in the bone marrow. Interestingly, the higher doses of dried plum did suppress the number of lymphoblasts, despite the fact that that the increase in this population due to OVX did not reach the level of statistical significance. This finding indicates that dried plum may affect the differentiation of cells further upstream from the lymphocyte populations observed here, such as pluripotent stem cells; however, this is a premature conclusion at this stage. Future studies should consider the alterations in T- and B-cell populations in peripheral sites such as the spleen and thymus in addition to the bone marrow.

The activation of various immune cell populations may also provide further explanation as to dried plum's mechanism of action as it relates to bone health. Chronic activation of the immune system, or inflammation, is known to play a significant role in bone metabolism and a number of pro-inflammatory cytokines (i.e., TNF-α, IL-1β and IL-6) regulate these processes [30]. For example, *in vitro* TNF-α and IL-6 initiate osteoclast differentiation and promote osteoclast activity in addition to inhibiting both osteoblastogenesis and osteoblast activity [17,31]. In this study, we observed that ovarian hormone deficiency increased *ex vivo* splenocyte activation, as indicated by increased TNF-α secretion when stimulated by the lymphocyte mitogen Con A. Splenocytes cultured from animals consuming the two diets supplemented with 15% and 25% dried plum (i.e., MDP and HDP) for 4 weeks exhibited a significantly diminished response to Con A (i.e., TNF-α production). No alterations in IL-6 with Con A stimulation or TNF-α were observed in splenocytes challenged with LPS *ex vivo*. These results indicate that dried plum decreases monocyte and T-cell activation *in vivo*. Because activated T cells are known to serve as a significant source of both TNF-α and RANKL which promote osteoclast differentiation and activity [21], further studies will be required to determine whether this is the underlying mechanism involved in the prevention of OVX-induced bone loss with dried plum.

In conclusion, our results show that dried plum's ability to protect C57BL/6J mice from skeletal loss induced by gonadal hormone deficiency could be explained by a decrease in bone resorption and formation. These changes in bone metabolism coincided with alterations in myeloid and lymphoid populations in the bone marrow and suppression of the immune cell activation. Our findings suggest that dietary supplementation with dried plum may have the potential to alter osteoclast and osteoblast precursor cell differentiation. Further studies are needed to advance our understanding of dried plum effects on bone marrow populations, especially as they related to osteoclast and osteoblast precursor cells, and the role of immune cell activation.

References

[1] Cummings SR, Melton LJ. Epidemiology and outcomes of osteoporotic fractures. Lancet 2002;359:1761–7.
[2] Bone Health and Osteoporosis: A Surgeon General's Report (2004). U.S. Department of Health and Human Services.
[3] Arjmandi BH, Lucas EA, Juma S, Soliman A, Stoecker BJ, Khalil DA, et al. Dried plum prevents ovariectomy-induced bone loss in rats. JANA 2001;4:50–6.
[4] Franklin M, Bu SY, Lerner MR, et al. Dried plum prevents bone loss in a male osteoporosis model via IGF-I and the RANK pathway. Bone 2006;39:1331–42.
[5] Deyhim F, Stoecker BJ, Brusewitz GH, Devareddy L, Arjmandi BH. Dried plum reverses bone loss in an osteopenic rat model of osteoporosis. Menopause 2005;12:755–62.
[6] Bu SY, Lucas EA, Franklin M, et al. Comparison of dried plum supplementation and intermittent PTH in restoring bone in osteopenic orchidectomized rats. Osteoporos Int 2007;18:931–42.
[7] Stacewicz-Sapuntzakis M, Bowen PE, Hussain EA, Mayanti-Wood BI, Farnsworth NR. Chemical composition and potential health effects of prunes: a functional food? Crit Rev Food Sci Nutr 2001;41:251–86.
[8] Cashman KD. A prebiotic substance persistently enhances intestinal calcium absorption and increases bone mineralization in young adolescents. Nutr Rev 2006;64:189–96.
[9] Gundberg CM. Vitamin K and bone: past, present, and future. J Bone Miner Res 2009;24:980–2.
[10] Sellmeyer DE, Schloetter M, Sebastian A. Potassium citrate prevents increased urine calcium excretion and bone resorption induced by a high sodium chloride diet. J Clin Endocrinol Metab 2002;87:2008–12.
[11] Bu SY, Hunt TS, Smith BJ. Dried plum polyphenols attenuate the detrimental effects of TNF-alpha on osteoblast function coincident with up-regulation of Runx2, Osterix and IGF-I. J Nutr Biochem 2008.
[12] Bu SY, Lerner M, Stoecker BJ, et al. Dried plum polyphenols inhibit osteoclastogenesis by downregulating NFATc1 and inflammatory mediators. Calcif Tissue Int 2008.
[13] Clowes JA, Riggs BL, Khosla S. The role of the immune system in the pathophysiology of osteoporosis. Immunol Rev 2005;208:207–27.
[14] Pacifici R, Rifas L, Teitelbaum S, et al. Spontaneous release of interleukin 1 from human blood monocytes reflects bone formation in idiopathic osteoporosis. Proc Natl Acad Sci U S A 1987;84:4616–20.
[15] Girasole G, Jilka RL, Passeri G, et al. 17 beta-Estradiol inhibits interleukin-6 production by bone marrow-derived stromal cells and osteoblasts in vitro: a potential mechanism for the antiosteoporotic effect of estrogens. J Clin Invest 1992;89:883–91.
[16] Jilka RL, Hangoc G, Girasole G, et al. Increased osteoclast development after estrogen loss: mediation by interleukin-6. Science 1992;257:88–91.
[17] Wei S, Kitaura H, Zhou P, Ross FP, Teitelbaum SL. IL-1 mediates TNF-induced osteoclastogenesis. J Clin Invest 2005;115:282–90.
[18] Manolagas SC. Birth and death of bone cells: basic regulatory mechanisms and implications for the pathogenesis and treatment of osteoporosis. Endocr Rev 2000;21:115–37.
[19] de Vries TJ, Schoenmaker T, Hooibrink B, Leenen PJ, Everts V. Myeloid blasts are the mouse bone marrow cells prone to differentiate into osteoclasts. J Leukoc Biol 2009;85:919–27.

[20] Cenci S, Weitzmann MN, Roggia C, et al. Estrogen deficiency induces bone loss by enhancing T-cell production of TNF-alpha. J Clin Invest 2000;106:1229–37.
[21] Weitzmann MN, Cenci S, Rifas L, Haug J, Dipersio J, Pacifici R. T cell activation induces human osteoclast formation via receptor activator of nuclear factor kappaB ligand-dependent and -independent mechanisms. J Bone Miner Res 2001;16:328–37.
[22] Li Y, Toraldo G, Li A, et al. B cells and T cells are critical for the preservation of bone homeostasis and attainment of peak bone mass in vivo. Blood 2007;109: 3839–48.
[23] Keyak JH, Meagher JM, Skinner HB, Mote Jr CD. Automated three-dimensional finite element modelling of bone: a new method. J Biomed Eng 1990;12:389–97.
[24] Kuvibidila S, Yu L, Ode D, Velez M, Gardner R, Warrier RP. Effects of iron deficiency on the secretion of interleukin-10 by mitogen-activated and non-activated murine spleen cells. J Cell Biochem 2003;90:278–86.
[25] Kuvibidila S, Baliga BS, Gardner R, et al. Differential effects of hydroxyurea and zileuton on interleukin-13 secretion by activated murine spleen cells: implication on the expression of vascular cell adhesion molecule-1 and vasoocclusion in sickle cell anemia. Cytokine 2005;30:213–8.
[26] Harkonen PL, Vaananen HK. Monocyte–macrophage system as a target for estrogen and selective estrogen receptor modulators. Ann N Y Acad Sci 2006; 1089:218–27.
[27] Smithson G, Beamer WG, Shultz KL, Christianson SW, Shultz LD, Kincade PW. Increased B lymphopoiesis in genetically sex steroid-deficient hypogonadal (hpg) mice. J Exp Med 1994;180:717–20.
[28] Masuzawa T, Miyaura C, Onoe Y, et al. Estrogen deficiency stimulates B lymphopoiesis in mouse bone marrow. J Clin Invest 1994;94:1090–7.
[29] Benayahu D, Shur I, Ben-Eliyahu S. Hormonal changes affect the bone and bone marrow cells in a rat model. J Cell Biochem 2000;79:407–15.
[30] Droke EA, Hager KA, Lerner MR, et al. Soy isoflavones avert chronic inflammation-induced bone loss and vascular disease. J Inflamm (Lond) 2007;4:17.
[31] Goldring SR. Inflammatory mediators as essential elements in bone remodeling. Calcif Tissue Int 2003;73:97–100.